*Solid-State Electronics* Vol. 35, No. 2, pp. 125–129, 1992
Printed in Great Britain. 

0038-1101/92 $5.00 + 0.00


# UNIFIED APPARENT BANDGAP NARROWING IN *n*- AND *p*-TYPE SILICON

D. B. M. KLAASSEN, J. W. SLOTBOOM and H. C. DE GRAAFF
Philips Research Laboratories, P.O. Box 80000, 5600 JA Eindhoven, The Netherlands

*(Received 20 May 1991; in revised form 23 July 1991)*

**Abstract**—In the literature, separate models exist for the apparent bandgap narrowing in *n*- and *p*-type Si, yielding a smaller bandgap narrowing in *n*-type than in *p*-type Si. Using a recently-published model, which describes both the majority and the minority carrier mobility, we have recalculated the apparent bandgap narrowing from the measurements upon which the bandgap narrowing models mentioned above are based. The results of this new interpretation show no difference in apparent bandgap narrowing in *n*- and *p*-type Si. A function describing the unified bandgap narrowing is presented.

## 1. INTRODUCTION

In 1976 the first empirical expression for the apparent bandgap narrowing in Si, which was derived from measurements of collector currents of *npn*-transistors, so for *p*-type Si, was introduced by Slotboom and de Graaff[1]. After about one decade in which many experiments on bandgap narrowing were published[2–5], del Alamo *et al.* presented an empirical expression for the apparent bandgap narrowing in *n*-type Si which was based on new experiments as well as on these data from the literature[6,7]. This expression yielded values about 35 mV smaller than those obtained from the expression of Slotboom and de Graaff. When Swirhun *et al.*[8] reported their experiments on *p*-type Si to be in agreement with the Slotboom–de Graaff expression, the opinion took root that the apparent bandgap narrowing is smaller in *n*-type than in *p*-type Si.

The minority carrier mobility plays a crucial role in the interpretation of most of the experiments on apparent bandgap narrowing. Recently we published a model which accurately describes both majority and minority carrier mobilities, including their temperature dependence[9]. Here we use this mobility model to recalculate the apparent bandgap narrowing from the measurements upon which the bandgap narrowing models mentioned above are based.

## 2. CORRECTION PROCEDURES

In most experiments on apparent bandgap narrowing, $\mu n_{i,e}^2$ is actually determined (e.g. method 1 of Refs[1,6,8]). Herein $\mu$ is the minority carrier mobility given as a function of the impurity concentration $N$ by:

$$\mu = \mu_{min} + \frac{\mu_{max} - \mu_{min}}{1 + (N/N_1)^{\alpha}}, \quad (1)$$

and $n_{i,e}^2$ is the effective intrinsic carrier concentration given by:

$$n_{i,e}^2(N, T) = C_1 T^3 \exp\{-q[V_g - \Delta V_{g0}(N)]/kT\}. \quad (2)$$

In eqn (2) $\Delta V_{g0}(N)$ is the apparent bandgap narrowing, which is independent of temperature [10] and described by:

$$\Delta V_{g0}(N) = V_1 \left\{ \ln\left(\frac{N}{N_2}\right) + \sqrt{\left[\ln\left(\frac{N}{N_2}\right)\right]^2 + C_2} \right\}. \quad (3)$$

The parameters used by the different authors can be found in Table 1. Using eqns (2–3) and keeping $\mu n_{i,e}^2$ constant, the relation between the new (corrected) value for the apparent bandgap narrowing $\Delta V_{g0}^{new}$ and the reported value $\Delta V_{g0}^{rep}$ is found to be:

$$\Delta V_{g0}^{new} = \Delta V_{g0}^{rep} + \frac{kT}{q} \ln\left(\frac{\mu^{rep}}{\mu^{new}}\right) + \frac{kT}{q} \ln\left(\frac{C_1^{rep}}{C_1^{new}}\right). \quad (4)$$

In other experiments on apparent bandgap narrowing, the dependence of the collector current on the base–emitter voltage has been measured as a function of temperature (e.g. method 2 of Refs[1,11]). In those experiments the temperature dependence of the minority carrier mobility, $\mu \propto T^{-\gamma}$, was obtained from the base sheet resistance underneath the emitter. Our new mobility model predicts a temperature dependence of the minority carrier mobility which is distinctly different from that of the majority carrier mobility (see Fig. 6 of Ref.[9]). For majority carriers $\gamma$ decreases with increasing concentration from about 2.3 to 0, whereas for minority carriers a lower limit of about 1 is found. Consequently, also for those experiments a correction is necessary, which can be derived from eqn (10) of Ref.[1] using $\mu \propto T^{-\gamma}$:

$$\Delta V_{g0}^{new} = \Delta V_{g0}^{rep} + \frac{kT_m}{q}(\gamma_{rep} - \gamma_{new}), \quad (5)$$

where $T_m$ is chosen in the middle of the temperature region used in the experiments.

Table 1. Model parameters for mobility [eqn (1)], intrinsic carrier concentration [eqn (2)] and apparent bandgap narrowing [eqn (3)] used in the interpretation of the experimental data. For all data on apparent bandgap narrowing in $n$-type Si we used the values as reported by del Alamo *et al.*[6,7,12]

| | Slotbottom and de Graaff ($p$-type) | del Alamo *et al.* ($n$-type) | Swirhun *et al.* ($p$-type) | This work ($n$- and $p$-type) |
|---|---|---|---|---|
| $\mu_{max}$ ($cm^2 V^{-1} s^{-1}$) | 1360 | 500 | 1412 | — |
| $\mu_{min}$ ($cm^2 V^{-1} s^{-1}$) | 92 | 130 | 232 | — |
| $N_1$ ($cm^{-3}$) | $1.3 \times 10^{17}$ | $8.0 \times 10^{17}$ | $8.0 \times 10^{16}$ | — |
| $\alpha$ | 0.91 | 1.25 | 0.90 | — |
| $C_1$ ($cm^{-6} K^{-3}$) | $9.61 \times 10^{32}$ | $1.38 \times 10^{33}$ | $1.26 \times 10^{33}$ | $9.61 \times 10^{32}$ |
| $V_g$ (V) | 1.206 | 1.206 | 1.206 | 1.206 |
| $V_1$ (mV) | 9.0 | 9.35 | 9.0 | 6.92 |
| $N_2$ ($cm^{-3}$) | $1.0 \times 10^{17}$ | $7.0 \times 10^{17}$ | $1.0 \times 10^{17}$ | $1.3 \times 10^{17}$ |
| $C_2$ | 0.5 | 0 | 0.5 | 0.5 |

## 3. RESULTS AND DISCUSSION

As the goal of this paper is to investigate whether the apparent bandgap narrowing in $p$- and $n$-type Si has to be described by different parameter values in eqn (3), only the data on which these parameter values were based were corrected using eqns (4) or (5). The new values for the apparent bandgap narrowing calculated from the Slotboom and de Graaff data (method 1) for $p$-type Si are smaller due to the minority electron mobility which is larger than the majority electron mobility (see Figs 1 and 5). Also for the data obtained by Slotboom and de Graaff with method 2 the new values for the apparent bandgap narrowing are smaller due to the difference in temperature dependence between minority and majority mobility (see Fig. 6 of Ref.[9]). Compared to the data (original and collected from the literature) reported by del Alamo *et al.*[12] for $n$-type Si the new apparent bandgap narrowing values are larger (see Fig. 5). At high concentrations this is due to a difference in parameter $C_1$ for the intrinsic carrier concentration, while at low concentrations the difference in minority hole mobility is also important (see Fig. 2). The minority hole mobility used by del Alamo *et al.* is at low concentrations based on the data of Dziewior and Silber[13], who found at $10^{17}$ $cm^{-3}$ a minority hole mobility equal to the lattice scattering mobility. Their observations are in disagreement with those of Dannhäuser and Krausse, who have found that at this concentration electron–hole scattering reduces the mobility by a factor of two[19,20] (see Fig. 3). Our mobility model is based on a simultaneous interpretation of data on minority electron mobility, minority hole mobility and mobility data on electron–hole scattering (see Figs 1–3 and Ref.[9]). We performed additional model calculations to illustrate the disagreement mentioned above:

- The importance of electron–hole scattering for the description of the Dannhäuser–Krausse data[19,20] is clarified by a calculation omitting this effect (see Fig. 3). The calculations were performed with a lattice temperature increasing linearly with carrier concentration from 300 K at low concentrations to 500 K at $10^{18}$ $cm^{-3}$ (see Fig. 3). This temperature increase, which is noticeable only at concentrations larger than $10^{17}$ $cm^{-3}$, is quite realistic in view of the power dissipated at this concentration (400 W for 100 $\mu$s in 1 $mm^3$)[20].

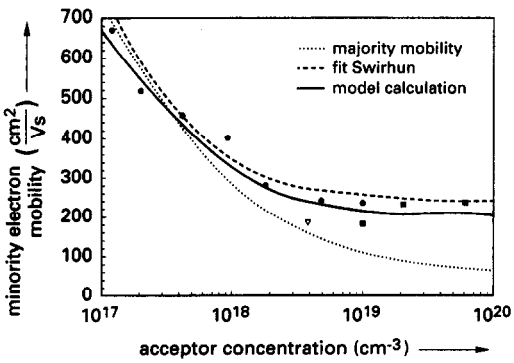


Fig. 1. Minority electron mobility as a function of the acceptor concentration: ● represent[13]; ▽ represent[14]; and ■ represent[8]. The fit of Swirhun *et al.*[8] (– – –); our new model[9] (——); and majority electron mobility as used by Slotboom and de Graaff[1] (· · · ·).

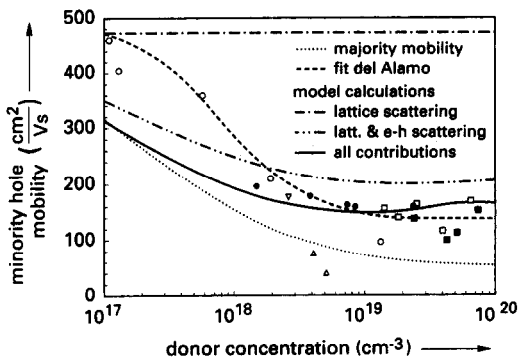


Fig. 2. Minority hole mobility as a function of the donor concentration: ○ represent[13] (a value of 615 $cm^2 V^{-1} s^{-1}$ reported at $4 \times 10^{17}$ $cm^{-3}$ is not included in this figure); ▽ represent[15]; △ represent[2]; □ represent[6,16]; ● represent[17]; and ■ represent[18]. The fit of del Alamo *et al.*[6,16] (– – –); our new model[9] including all contributions (——); our new model including only lattice scattering (— · —); our new model including lattice and electron–hole scattering (— · · —); and the majority hole mobility (· · · ·).

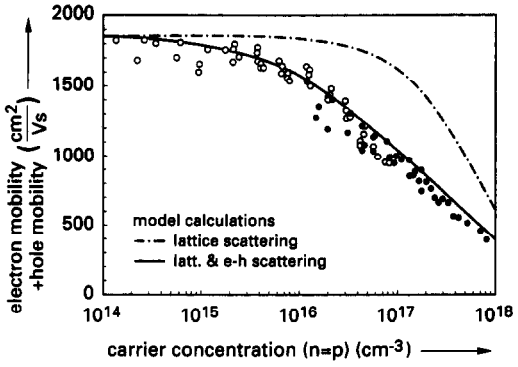


Fig. 3. Sum of electron and hole mobility as a function of carrier concentration. Symbols represent experimental data measured in the intrinsic region of a *pin* diode as function of the injected carrier concentration ($n = p$): ○ represent[19]; and ● represent[20]. Curves indicate model calculations with a temperature increasing linearly with carrier concentration from 300 K at low concentrations to 500 K at $10^{18}$ cm$^{-3}$: our new model[9] including all contributions (——); and our new model including only lattice scattering (— · —).

- Including only lattice scattering and electron–hole scattering in the calculation yields a minority hole mobility, that is already smaller than the data of Dzewior and Silber[13] (see Fig. 2).
- Including hole–donor scattering reduces the minority hole mobility even further (see Fig. 2).

From these observations it is clear that the data of Dziewior and Silber[13] below $10^{18}$ cm$^{-3}$ are in conflict with the data of Dannhäuser and Krausse[19,20]. The scatter in the data of Dziewior and Silber[13] is quite large: at a donor concentration of $4 \times 10^{17}$ cm$^{-3}$ a minority hole mobility of 615 cm$^2$ V$^{-1}$ s$^{-1}$ was reported (not included in Fig. 2), which is 145 cm$^2$ V$^{-1}$ s$^{-1}$ above the lattice scattering mobility being the upper limit. Consequently these data cannot be used to oppose that at a concentration of $10^{17}$ cm$^{-3}$, electron–hole scattering and hole–donor scattering will reduce the minority hole mobility to a value smaller than the lattice scattering mobility.

Correction [see eqn (5)] of the data for *p*-type Si of Ghannam[11] yields values which are in agreement with all the previous data. Recently a value for $C_1$ of $7.75 \times 10^{32}$ cm$^{-6}$ K$^{-3}$ has been suggested in the literature[21]. Use of this value would imply an increase of about 5 mV for all data corrected via eqn (4). Such an increase, however, is unimportant for the conclusion that all corrected data discussed so far lie close together, showing no difference in apparent bandgap narrowing between *p*- and *n*-type Si.

Swirhun *et al.* reported their experiments on *p*-type Si to be in agreement with Slotboom and de Graaff[8]. However, they used a minority electron mobility slightly larger than in our new model (and much larger than the majority electron mobility of Ref.[1]; see Fig. 1) and, moreover, a $C_1$-value in the model for the intrinsic carrier concentration that is larger than our value, so the corrected values for their

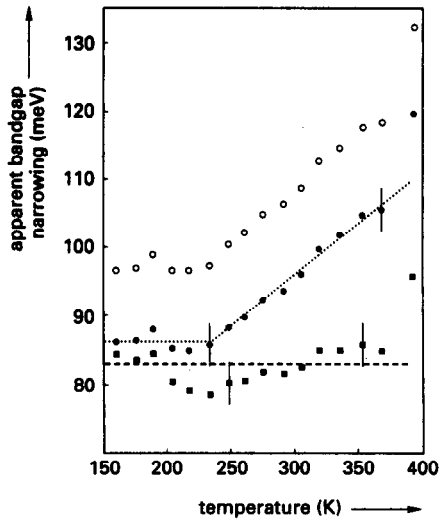


Fig. 4. Apparent bandgap narrowing in *p*-type Si as a function of temperature for an acceptor concentration of $2 \times 10^{19}$ cm$^{-3}$: data as reported by Swirhun *et al.*[22,23] (●); data corected for mobility and intrinsic carrier concentration [see eqn (4)] (○); and the data that is obtained if the epi-diffusion length is replaced by the bulk-diffusion length [see eqn (7)] (■). The dotted line and error bars are taken from[22,23].

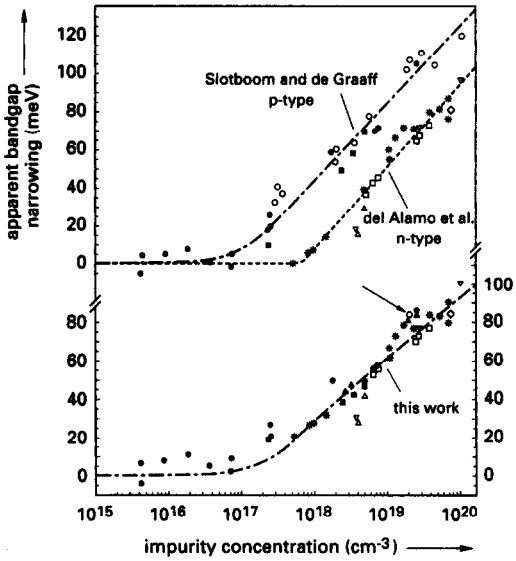


Fig. 5. In the upper part the apparent bandgap narrowing as reported in the literature is shown as a function of the impurity concentration. For *p*-type Si: ● represent[1]; ○ represent[8]; and ■ represent[11]. The fit of Slotboom and de Graaff[1] (· · · ·). For *n*-type Si △ represent[2]; □ represent[3]; ▽ represent[4]; ◇ represent[5]; and * represent[6,7,12]. It should be noted that only data considered in [6,7,12] is reproduced. The fit of del Alamo *et al.*[6,7] (– – –). In the lower part the corrected values for the apparent bandgap narrowing as a function of the impurity concentration are given (see text). Symbols represent the data as in the upper part; ▲ triangles represent the data of [25], that did not need to be corrected (see text). Note the corrected data of [8] at a concentration of $2 \times 10^{19}$ cm$^{-3}$ (arrow). Our new fit describing the apparent bandgap narrowing in both *n*- and *p*-type Si (— · —).

data are larger than the original ones (see Fig. 4). Consequently they lie about 40 mV higher than all other data in Fig. 5.

Swirhun *et al.* obtained their values for the apparent bandgap narrowing from the collector saturation current density, $J_{c0}$, of a vertical bipolar transistor fabricated in $p^+$ epimaterial (see Ref.[8] and eqn (6.23) of Ref.[22]):

$$J_{c0} = \frac{kT}{N_A} \frac{\mu_n n_{i,e}^2}{L_n' \sinh(W_B/L_n')}, \quad (6)$$

where $L_n'$ is the minority carrier diffusion length in the epimaterial measured on lateral $p^+$ epilayer transistors and $W_B$ is the vertical basewidth. Swirhun observes in these epi-devices smaller diffusion lengths ($L_n'$) than in their bulk-devices ($L_n$) used to determine the minority carrier mobility ($\mu_n$) (cf. Figs 6.9 and 6.20 of Ref.[22]). He indicates that the epi-devices are less well-suited for accurate determination of diffusion lengths due to the fact that "some current injected from the lateral emitter that might otherwise reach the collector is sunk at the epi–substrate junction." Nevertheless, he attributes the smaller diffusion lengths to lower lifetimes in the epi-devices[22], and still uses them in the interpretation of the bandgap narrowing experiments[8,23].

At the high dopant concentrations used by Swirhun *et al.* the lifetime is determined by Auger recombination and is therefore much less dependent on device processing than when it was determined by Shockley–Read–Hall recombination. Consequently lifetimes and diffusion lengths should be equal in epi- and bulk-devices. This leads to the conclusion that the diffusion lengths in the epimaterial measured by Swirhun *et al.* are smaller than the diffusion lengths obtained in the bulk material because of the possible systematic error indicated by those authors (see above). For the vertical bipolar transistor with an acceptor concentration of $2 \times 10^{19}$ cm$^{-3}$ the basewidth was published[8,22]. Consequently we can correct the apparent bandgap narrowing obtained by Swirhun *et al.* for the use of the wrong diffusion length [see eqn (6)]:

$$\Delta V_{g0}^{final} = \Delta V_{g0}^{new} + \frac{kT}{q} \ln\left[\frac{L_n \sinh(W_B/L_n)}{L_n' \sinh(W_B/L_n')}\right], \quad (7)$$

where $\Delta V_{g0}^{new}$ is the value obtained using eqn (4). The value obtained for the apparent bandgap narrowing at $2 \times 10^{19}$ cm$^{-3}$ is in good agreement with all other data (see Fig. 5). Moreover, application of the same procedure to the apparent bandgap narrowing data measured as function of temperature by Swirhun *et al.*[23] (see Fig. 4) yielded an apparent bandgap narrowing independent of temperature! This is in agreement with the conclusion of Slotboom[10], that between 280 and 400 K the apparent bandgap narrowing as used in eqn (2) is independent of temperature. It should also be noted that from optical data a bandgap narrowing independent of temperature can be concluded[24].

At this point it is interesting to mention some recent publications in this field. On $p$-type Si King and Swanson[25] have applied a method to determine the apparent bandgap narrowing independent of the intrinsic carrier concentration at low dopant concentrations [$C_1$ in eqn (2)]. Their data are in disagreement with the original data of Swirhun and lie closely together with all other corrected data (see Fig. 5). Based on theoretical calculations, Jain and Roulston[26] have developed a simple expression for the bandgap narrowing in heavily-doped Si at low temperatures. They need, however, the position of the Fermi level to find the apparent bandgap narrowing. Moreover, they add 17 meV to their results for $p$-type Si and 5 meV to their results for $n$-type Si in order to obtain agreement at high concentrations between their calculations and the uncorrected data shown in Fig. 5 for room temperature. They justify this "temperature correction" by a possible temperature dependence of the bandgap narrowing. It is interesting to note that without this "temperature correction" their results yield an apparent band narrowing for $p$-type Si slightly larger than that following from our expression and at most 15 meV larger than their results for $n$-type Si which are slightly smaller than that following from our expression.

All corrected data shown in Fig. 5 for the apparent bandgap narrowing in both $n$- and $p$-type Si can be fitted with new parameter values in the familiar expression [see Fig. 5, eqn (3) and Table 1]. In Fig. 6 a collection of experimentally determined $\mu_n \exp[\Delta E_{g0}/kT]$ values for $p$-type Si is shown as a function of the acceptor concentration (cf. Fig. 1 of Ref.[27]). These values were calculated from collector saturation currents measured on *npn*-transistors

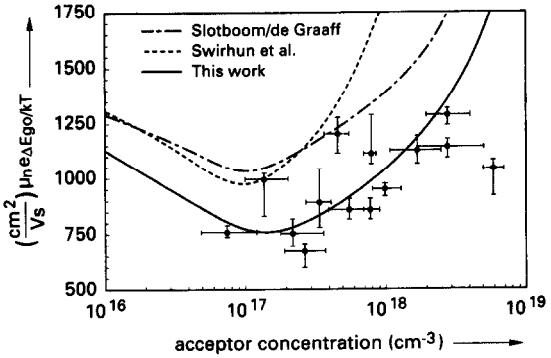


Fig. 6. Values of $\mu_n \exp(\Delta E_{g0}/kT)$ for $p$-type Si as a function of the acceptor concentration. The data was calculated from the collector saturation current as measured on *npn*-transistors fabricated in various processes. The chain-dashed line (– – –) is calculated using the electron majority mobility (see Table 1) and the bandgap narrowing model of Slotboom and de Graaff[1] (see also Table 1). The dashed line (– – – –) is calculated using the same bandgap narrowing model and the expression for the minority electron mobility of Swirhun *et al.*[8] (see also Table 1). The solid curve (——) is calculated using the new mobility model[9] and the new parameter values for the bandgap narrowing presented here (see also Table 1).

fabricated in various processes. The acceptor concentration was obtained from sheet resistance and capacitance measurements and from SIMS profiles. Using the new parameter values for the apparent bandgap narrowing together with our new mobility model, better agreement with these data is obtained than with existing models (see Fig. 6).

## 4. CONCLUSION

Using a new mobility model, the apparent bandgap narrowing in $n$- and $p$-type Si has been recalculated from published experiments. All new values for the apparent bandgap narrowing lie close together, eliminating differences between $n$- and $p$-type Si. Moreover, the apparent bandgap narrowing is shown to be independent of temperature. The new values for the apparent bandgap narrowing can be described by the familiar expression using new parameter values.

Using these new parameter values for the apparent bandgap narrowing together with our new mobility model a better agreement with experimental data on $\mu_n \exp[\Delta E_{g0}/kT]$ for $p$-type Si is obtained than with existing models.

*Acknowledgement*—Part of this work was funded by ESPRIT Project 2016.

## REFERENCES

1. J. W. Slotboom and H. C. de Graaff, *Solid-St. Electron.* **19,** 857 (1976).
2. R. P. Mertens, J. L. van Meerbergen, J. F. de Nijs and R. J. van Overstraeten, *IEEE Trans. Electron Devices* **ED-27,** 949 (1980).
3. A. W. Wieder, *IEEE Trans. Electron Devices* **ED-27,** 1402 (1980).
4. A. Neugroschel, S. C. Pao and F. A. Lindholm, *IEEE Trans. Electron Devices* **ED-29,** 894 (1982).
5. G. E. Possin, M. S. Adler and B. J. Baliga, *IEEE Trans. Electron Devices* **ED-31,** 3 (1984).
6. J. del Alamo, S. Swirhun and R. M. Swanson, *IEDM Tech. Dig.*, p. 290 (1985).
7. J. del Alamo and R. M. Swanson, *IEEE Trans. Electron Devices* **ED-34,** 1580 (1987).
8. S. E. Swirhun, Y.-H. Kwark and R. M. Swanson, *IEDM Tech. Dig.*, p. 24 (1986).
9. D. B. M. Klaassen, *IEDM Tech. Dig.*, p. 357 (1990).
10. J. W. Slotboom, *Solid-St. Electron.* **20,** 279 (1977).
11. M. Y. Ghannam, Ph.D. Dissertation, Katholieke Universiteit Leuven (1985).
12. J. del Alamo, S. Swirhun and R. M. Swanson, *Solid-St. Electron.* **28,** 47 (1985).
13. J. Dziewior and D. Silber, *Appl. Phys. Lett.* **35,** 170 (1979).
14. D. D. Tang, F. F. Fang, M. Scheuermann, T. C. Chen and G. Sai-Halasz, *IEDM Tech. Dig.*, p. 20 (1986).
15. D. E. Burk and V. de la Torre, *IEEE Electron Device Lett.* **5,** 231 (1984).
16. S. W. Swirhun, J. A. del Alamo and R. M. Swanson, *IEEE Electron Device Lett.* **7,** 168 (1986).
17. C. H. Wang, K. Misiakos and A. Neugroschel, *IEEE Trans. Electron Devices* **ED-37,** 1314 (1990).
18. C. H. Wang and A. Neugroschel, *IEEE Electron Device Lett.* **11,** 576 (1990).
19. F. Dannhäuser, *Solid-St. Electron.* **15,** 1371 (1972).
20. J. Krausse, *Solid-St. Electron.* **15,** 1377 (1972).
21. M. A. Green, *J. appl. Phys.* **67,** 2944 (1990).
22. S. E. Swirhun, Ph.D. Dissertation, Stanford University (1987).
23. S. E. Swirhun, D. E. Kane and R. M. Swanson, *IEDM Tech. Dig.*, p. 298 (1988).
24. J. Wagner and J. A. del Alamo, *J. appl. Phys.* **63,** 425 (1988).
25. R. R. King and R. M. Swanson, *IEEE Trans. Electron Devices* **ED-38,** 1399 (1991).
26. S. C. Jain and D. J. Roulston, *Solid-St. Electron.* **34,** 453 (1991).
27. H. C. de Graaff and G. A. M. Hurkx, *Proc. ESSDERC'87*, Bologna, pp. 503–506 (1987).